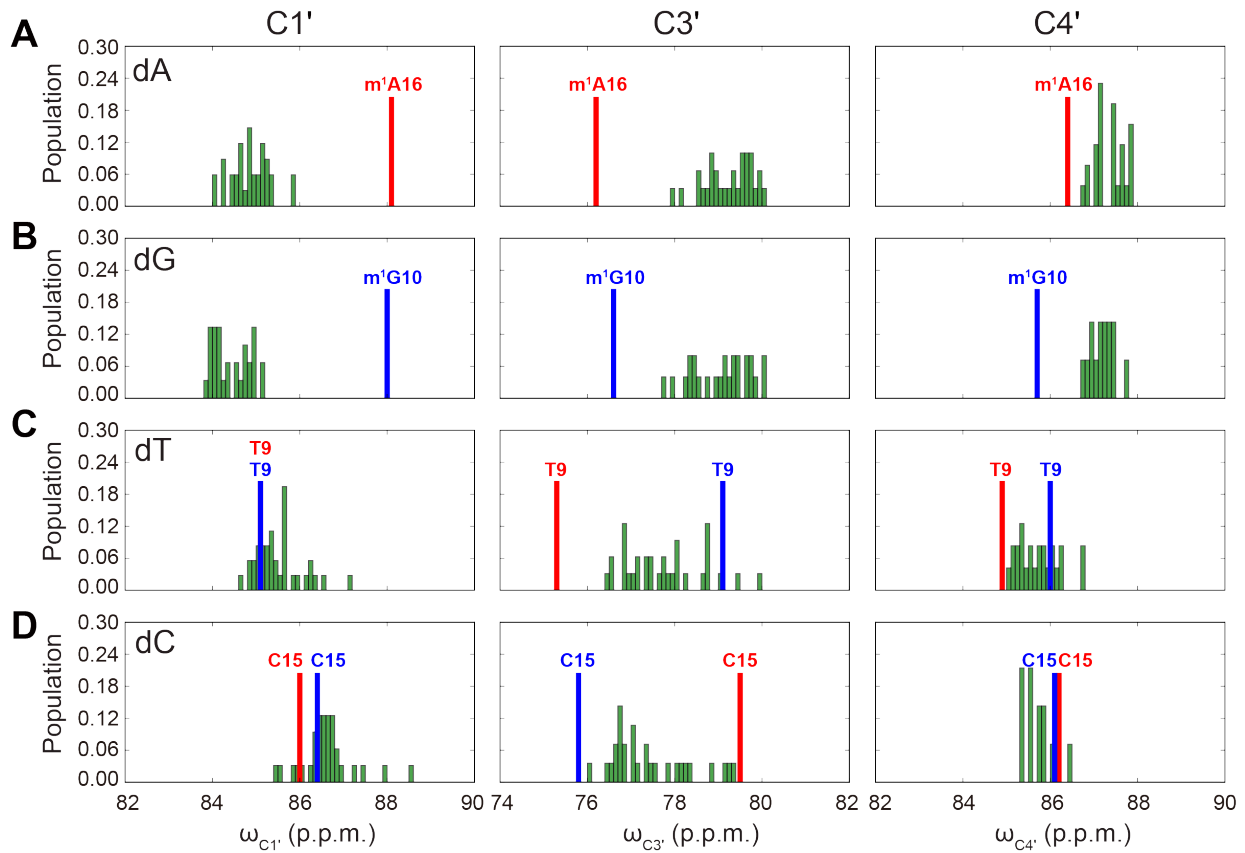


**Atomic Structures of Excited State A-T Hoogsteen Base Pairs in Duplex DNA by
Combining NMR Relaxation Dispersion, Mutagenesis, and Chemical Shift Calculations**

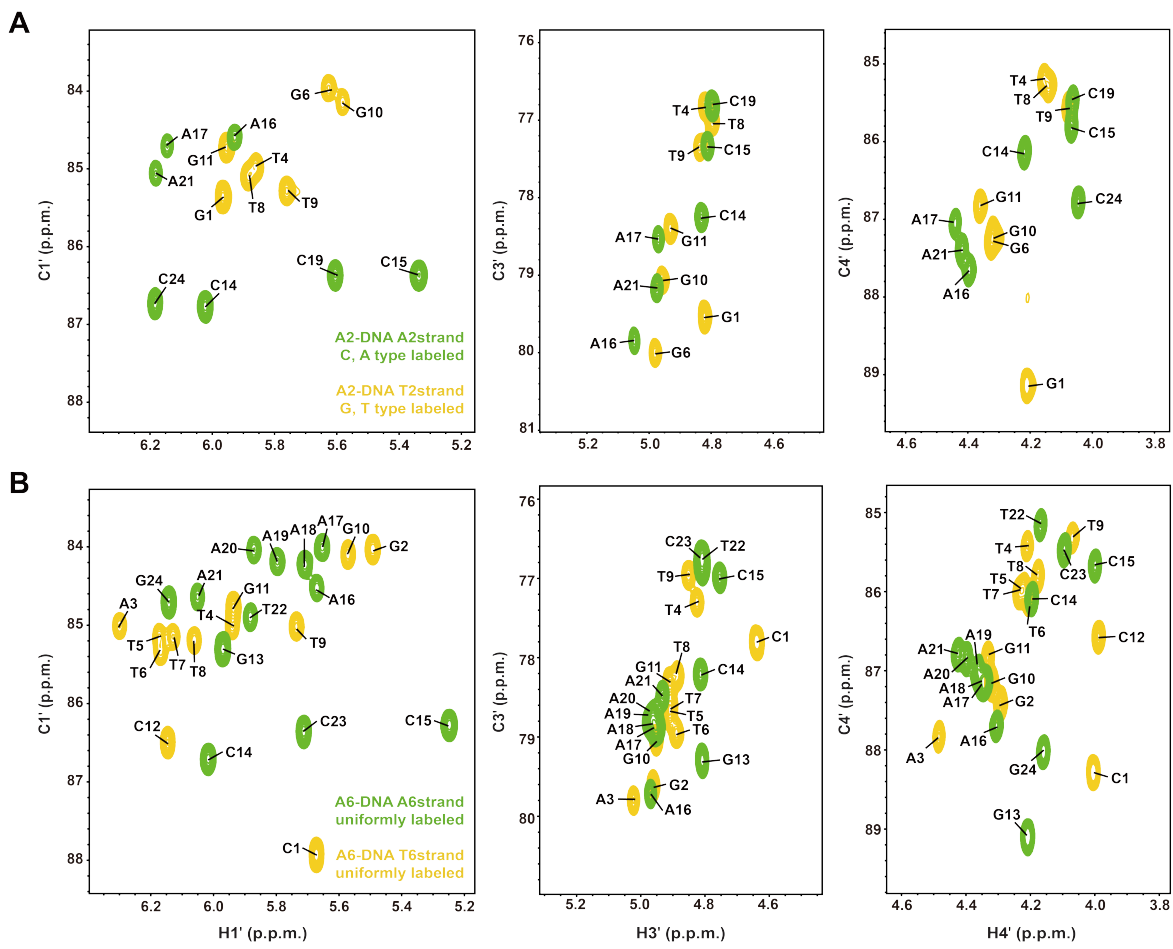
Honglue Shi¹, Mary C. Clay², Atul Rangadurai², Bharathwaj Sathyamoorthy^{1,2}, David A. Case^{3*},
and Hashim M. Al-Hashimi^{1,2,*}

Supplementary Information

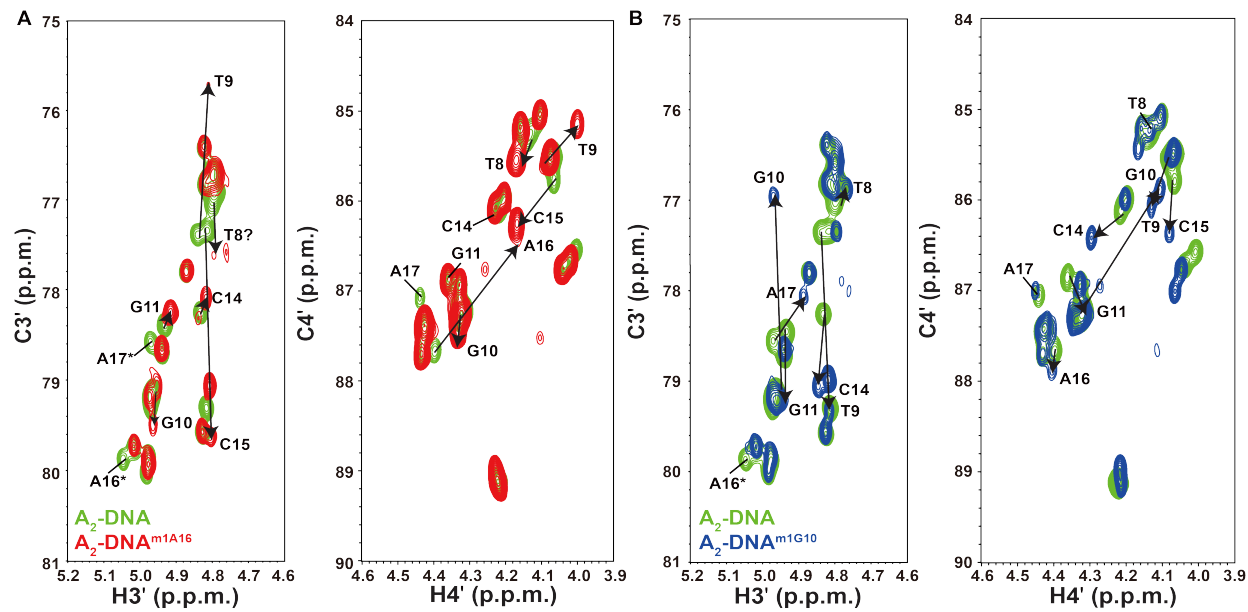
Supplementary Figures



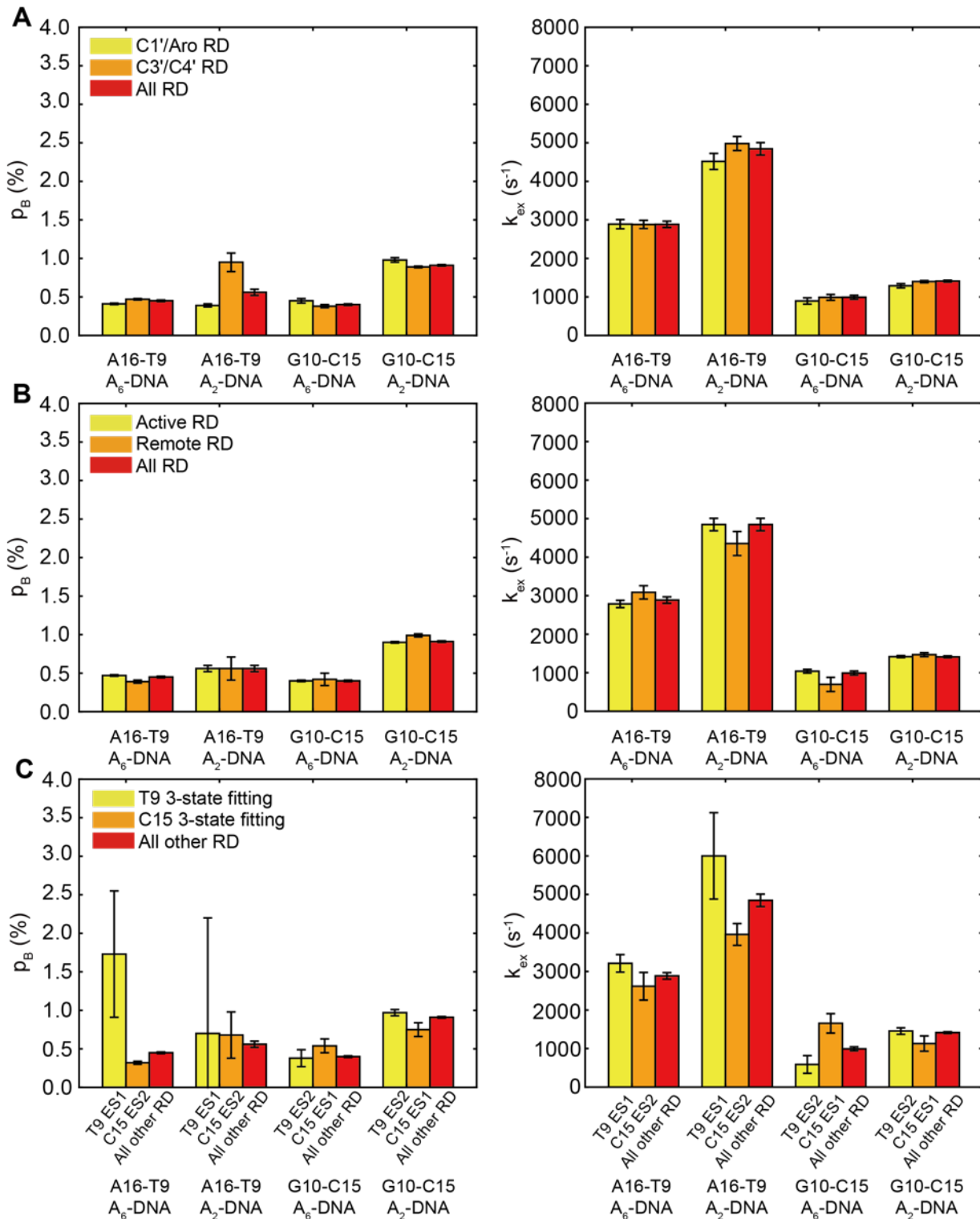
Supplementary Figure 1. Deoxyribose C1', C3', C4' chemical shift distribution for (A) dA (B) dG (C) dT and (D) dC in canonical duplex DNA from nine entries in BMRB¹. The sugar chemical shifts of m¹A16, T9, C15 in A₆-DNA^{m1A16} (red) and m¹G10, C15, T9 in A₆-DNA^{m1G10} (blue) are also shown on the histogram.



Supplementary Figure 2. (A) Residue-type $^{13}\text{C}/^{15}\text{N}$ labeled A₂-DNA improves spectral resolution for RD measurement. (B) Uniformly $^{13}\text{C}/^{15}\text{N}$ labeled A₆-DNA.

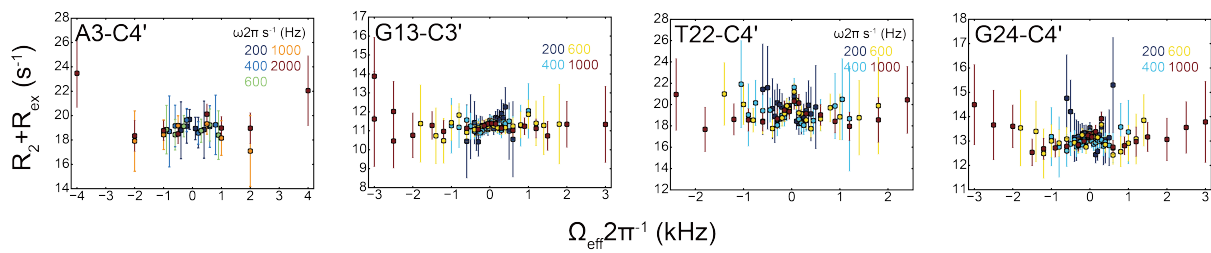


Supplementary Figure 3. Overlays of 2D C3'-H3' and C4'-H4' HSQC spectra for A₂-DNA (green) with (A) A₂-DNA^{m1A16} (red) and (B) A₂-DNA^{m1G10} (blue).

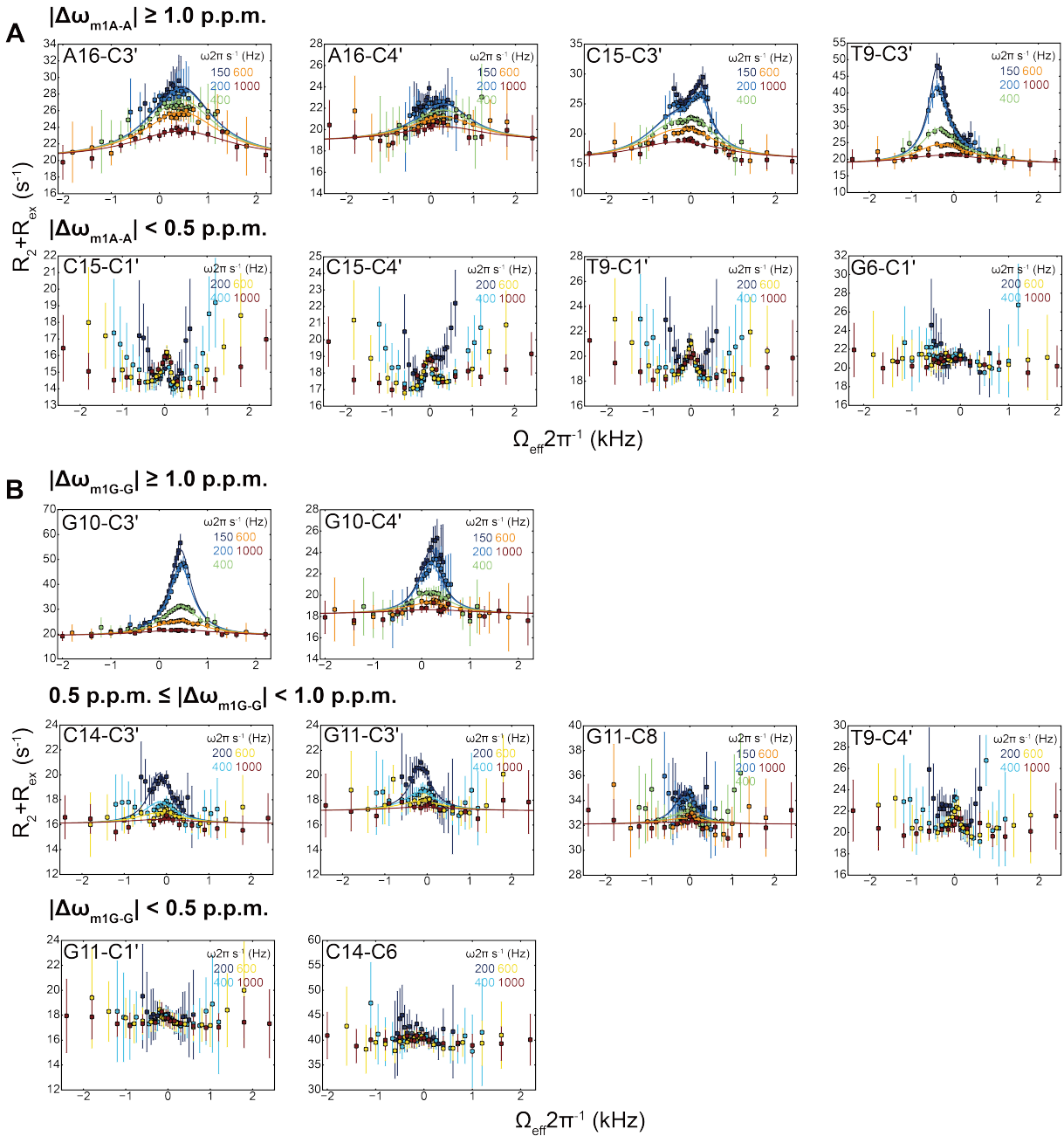


Supplementary Figure 4. Comparison of exchange parameters deduced using different RD datasets. (A) Comparison of exchange parameters deduced from fitting RD data measured at A16-T19 and G10-C15 bp. Shown are the exchange parameters deduced based on fitting C1'

and aromatic RD (yellow), C3' and C4' RD (orange), and all RD data combined (red). (B) Comparison of exchange parameters deduced based on active RD (yellow), remote RD (orange), and all RD (red). (C) Comparison of exchange parameters deduced based on 3-state fitting T9 (yellow) and C15 (orange), versus those obtained from fitting all other RD data (red). Exchange parameters for T9 ES1 and C15 ES2 are compared to those obtained for A16-T9 Hoogsteen based on all other RD data while those of T9 ES2 and C15 ES1 are compared to those obtained for G10-C⁺15 Hoogsteen based on all other RD data.

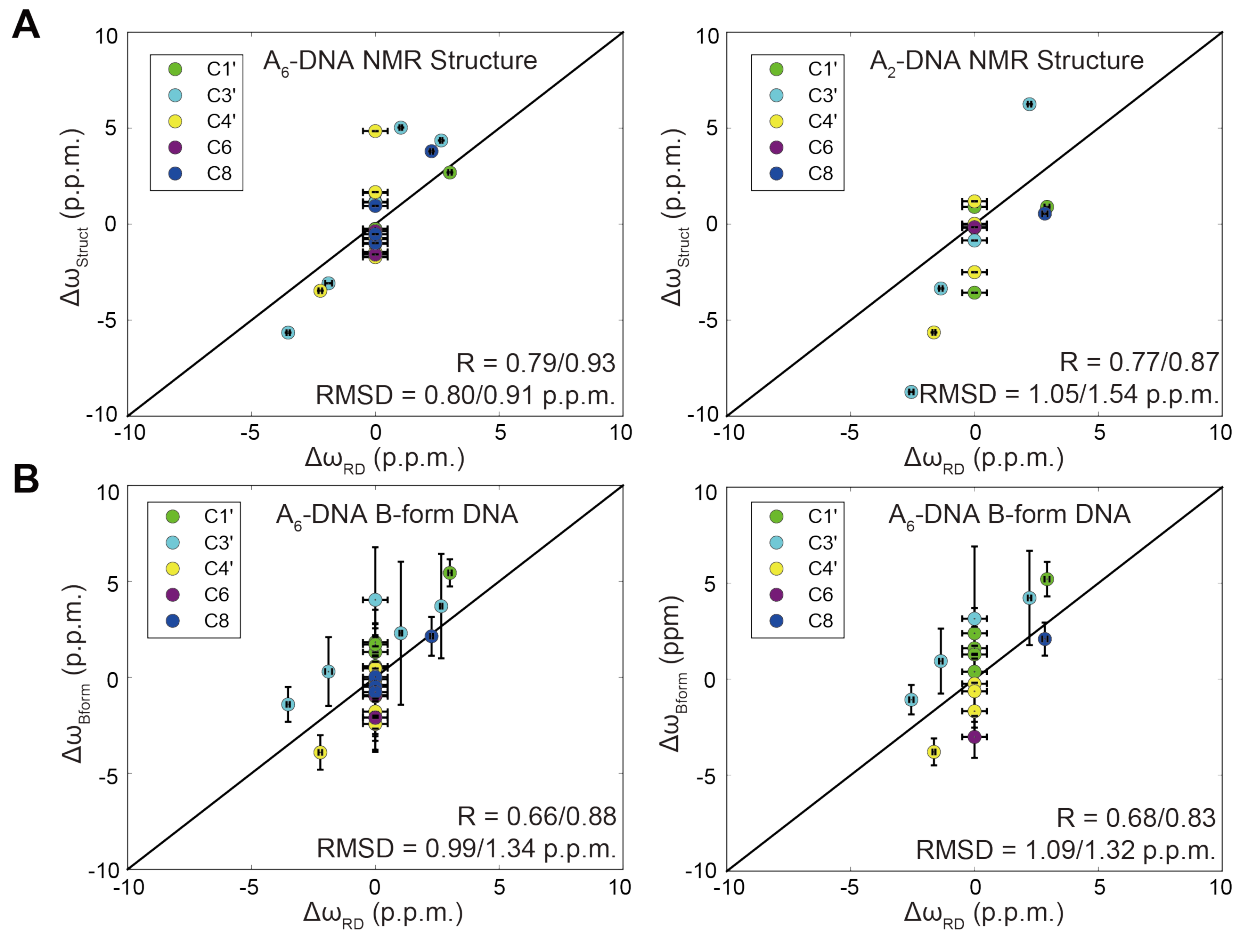


Supplementary Figure 5. All other flat RD profiles of A₆-DNA at pH 6.8. Shown are all other flat RD profiles of A₆-DNA at pH 6.8.

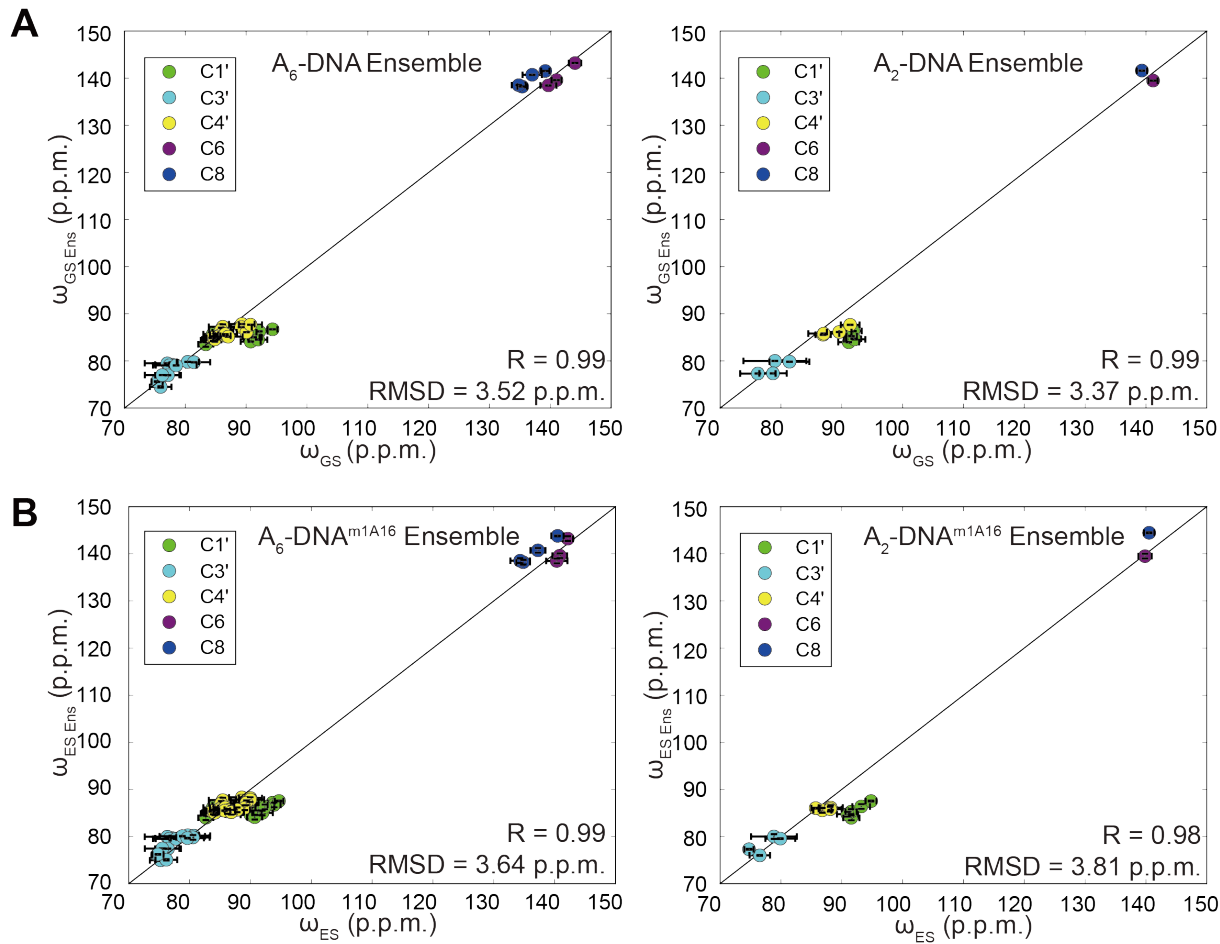


Supplementary Figure 6. Shown are all ^{13}C off-resonance R1 ρ RD profiles with best global fit of A₂-DNA measured at (A) highlighting A16-T9 Hoogsteen bp exchange and (B) highlighting G10-C⁺15 Hoogsteen bp exchange both at pH 5.4 and 25 °C. Error bars represent experimental uncertainty (one s.d., see Methods). Also shown are the differences in chemical shifts $\Delta\omega$ between Watson-Crick and Hoogsteen predicted based on comparison of chemical shifts

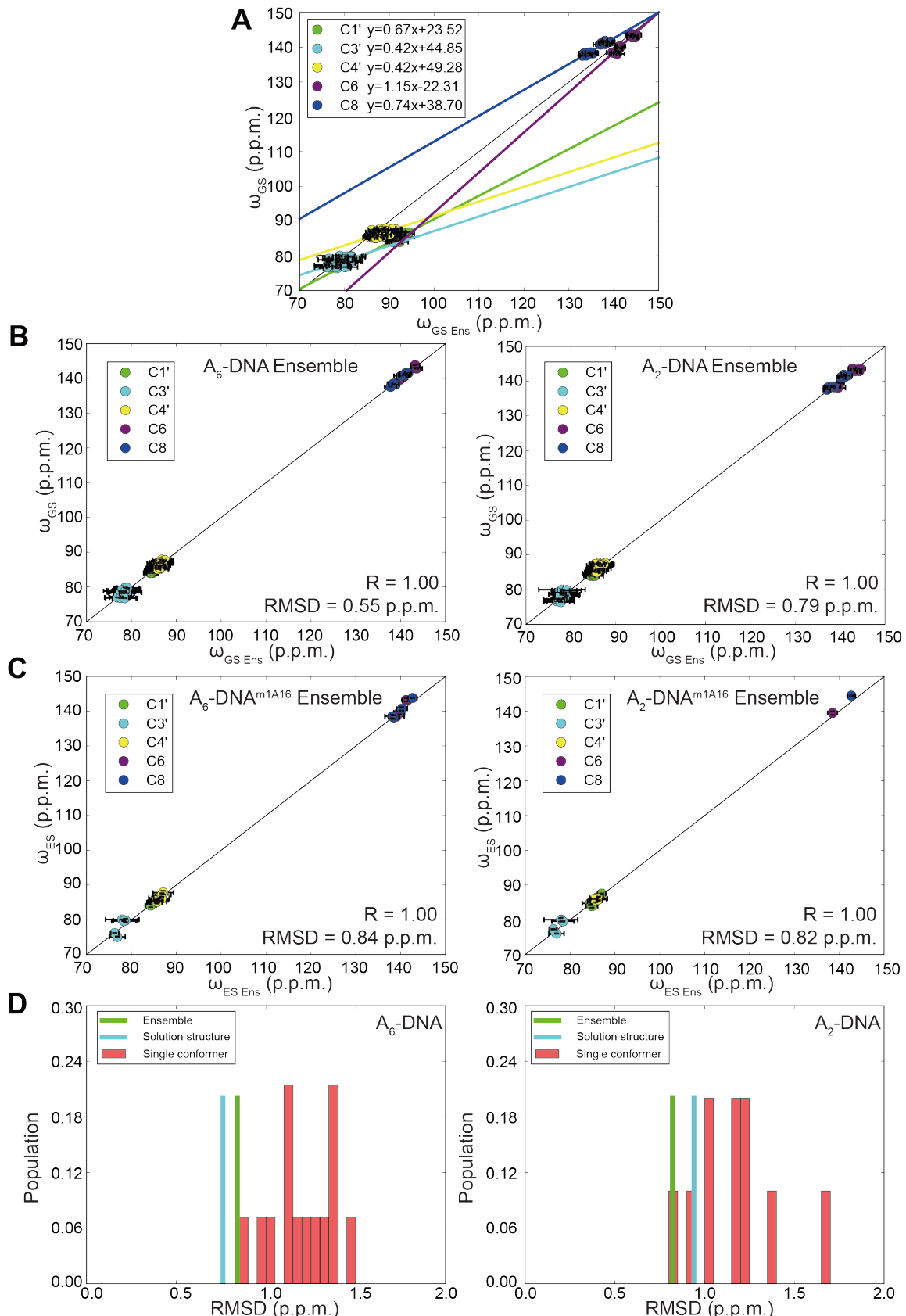
measured in the m¹A and m¹G stabilizing mutants with the unmodified duplexes. RD is not expected for $|\Delta\omega_{m1A-A}|$ or $|\Delta\omega_{m1G-G}| < 0.5$ p.p.m. ($|\Delta\omega_{m1A-A}| = |\omega_{m1A} - \omega_A|$ and $|\Delta\omega_{m1G-G}| = |\omega_{m1G} - \omega_G|$) whereas it is expected for $|\Delta\omega_{m1A-A}|$ or $|\Delta\omega_{m1G-G}| > 1.0$ p.p.m. and $|\Delta\omega_{m1A-A}|$ or $|\Delta\omega_{m1G-G}|$ between 0.5 to 1.0 p.p.m. may or may not lead to detectable RD depending the quality of the data and the exchange parameters.



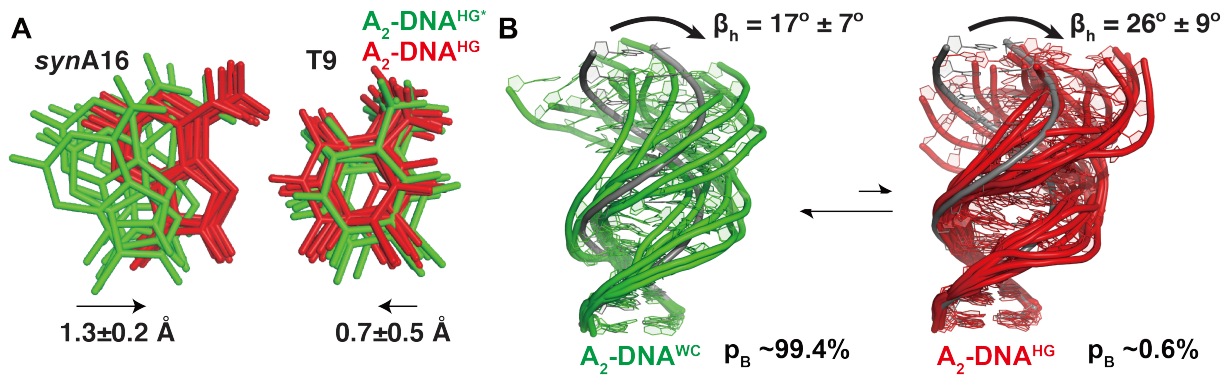
Supplementary Figure 7. Comparison of $\Delta\omega_{RD} = \omega_{ES} - \omega_{GS}$ measured by RD with values obtained from the differences in chemical shifts predicted based on the (A) NMR structures and (B) idealized B-form DNA of the modified and unmodified duplexes i.e. $\Delta\omega_{calc} = \omega_{calc-m1A} - \omega_{calc-A}$ in A₂-DNA and A₆-DNA.



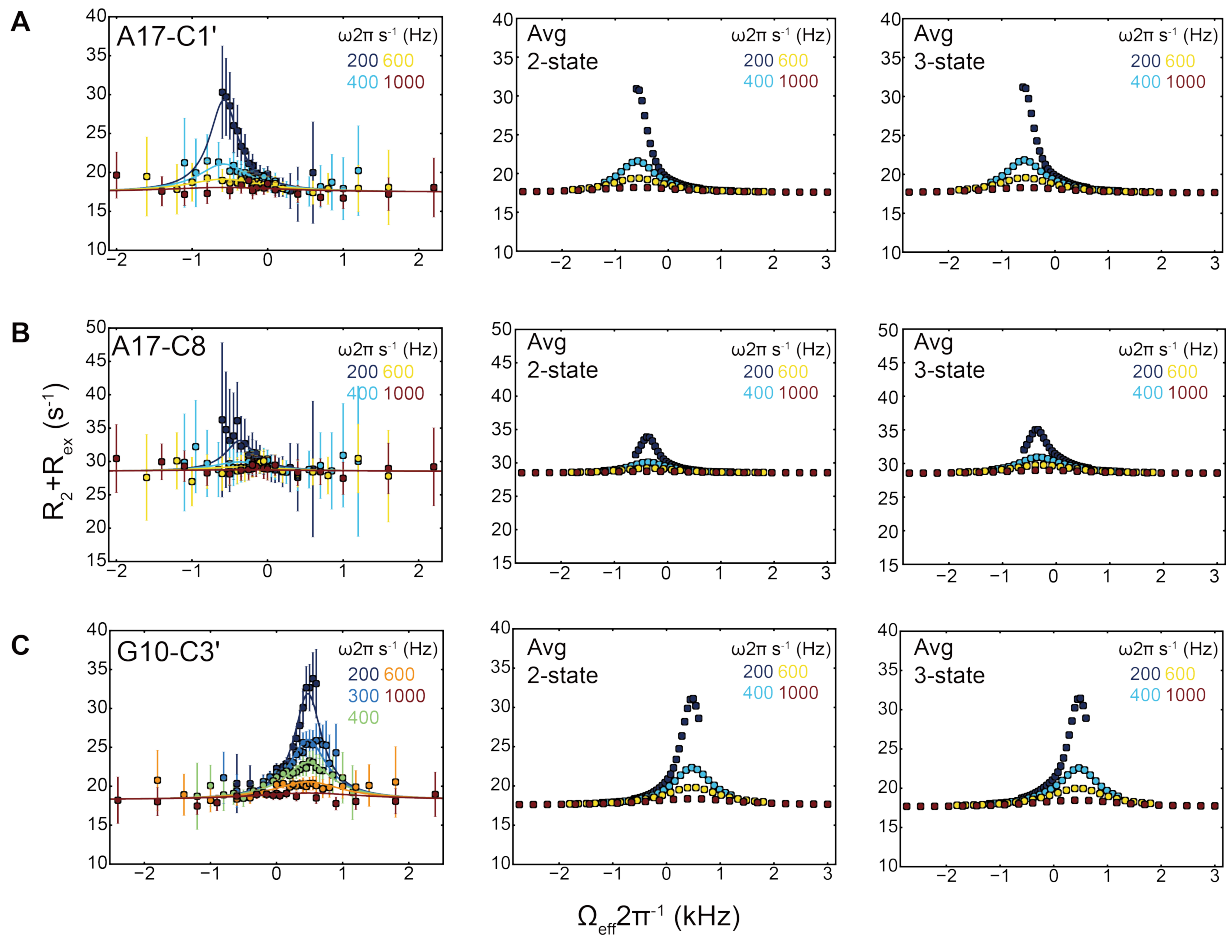
Supplementary Figure 8. Comparison of chemical shifts (ω) measured for the GS (ω_{GS}) or ES ($\omega_{ES} = \omega_{GS} + \Delta\omega_{RD}$) with values obtained from the chemical shifts predicted based on the ensemble structures ($\omega_{GS\text{Ens}}$ or $\omega_{ES\text{Ens}}$) without applying any correction for the (A) unmodified (GS) and (B) modified (ES) duplexes for A_2 - and A_6 -DNA.



Supplementary Figure 9. (A) Comparison of chemical shifts (ω) measured for the GS (ω_{GS}) versus predicted chemical shifts ($\omega_{GS\ Ens}$) for different spin types in A₂-DNA and A₆-DNA ensemble structures. The predicted values are averaged over the ensemble of conformers in unmodified A₂-DNA and A₆-DNA. (B) As in (A) following correction of the predicted values through linear fitting of predicted $\omega_{GS\ Ens}$ to measured ω_{GS} yielding a slope and intercept for each type of nuclei shown in (A). A correction was then applied by multiplying the predicted value by the slope followed by addition of the intercept i.e. $y = k*x + b$ (k is slope and b is intercept). Comparison of ω_{GS} measured in GS with values obtained from the chemical shifts predicted $\omega_{GS\ Ens}$ based on the ensembles structures of the unmodified duplexes in A₂-DNA and A₆-DNA with linear correction. (C) Comparison of measured chemical shift of ES ($\omega_{ES} = \omega_{GS} + \Delta\omega_{RD}$) by adding $\Delta\omega_{RD}$ measured by RD and ω_{GS} measured in GS with values obtained from the chemical shifts predicted $\omega_{ES\ Ens}$ based on the ensembles structures of the modified duplexes in A₂-DNA and A₆-DNA with linear correction. (D) Histogram showing the root-mean-square-deviation (RMSD) between ω_{meas} and ω_{calc} when using different input structures and ensemble to compute ω_{calc} : dynamic ensembles (green), solution structures (cyan), and every conformer in the ES-ensemble (red) with linear correction.



Supplementary Figure 10. (A) Comparison of A_2 -DNA (green) and $A_2\text{-DNA}^{\text{m1A16}}$ (red) ensembles showing translation of *synA16* towards the complementary strand. The A16 in A_2 -DNA was flipped into a *syn* conformation to aid comparison. (B) Previously reported ensembles² of the GS A_2 -DNA (green) and ES-mimic $A_2\text{-DNA}^{\text{m1A16}}$ (red) showing global changes in structure and dynamics accompanying formation of Hoogsteen bps. An idealized B-form DNA helix (in gray) is overlaid for reference.



Supplementary Figure 11. Comparison of measured off-resonance RD profiles with profiles simulated using Bloch-McConnell simulations assuming only active RD (2-state) or both active and remote RD (3-state) for (A) A17 C1', (B) A17 C8 and (C) G10 C3'. The simulations assumed the followed exchange parameters: A17 C1' ES1 (active) is $p_B = 0.03\%$, $k_{ex} = 700\text{ s}^{-1}$, $\Delta\omega = 3.3\text{ p.p.m.}$ and ES2 (remote) is $p_B = 0.05\%$, $k_{ex} = 3000\text{ s}^{-1}$, $\Delta\omega = 0.6\text{ p.p.m.}$; A17 C8 ES1 (active) is $p_B = 0.03\%$, $k_{ex} = 700\text{ s}^{-1}$, $\Delta\omega = 2.0\text{ p.p.m.}$ and ES2 (remote) is $p_B = 0.05\%$, $k_{ex} = 3000\text{ s}^{-1}$, $\Delta\omega = 1.0\text{ p.p.m.}$; G10 C3' ES1 (active) is $p_B = 0.4\%$, $k_{ex} = 1000\text{ s}^{-1}$, $\Delta\omega = -2.7\text{ p.p.m.}$ and ES2 (remote) is $p_B = 0.5\%$, $k_{ex} = 3000\text{ s}^{-1}$, $\Delta\omega = 0.6\text{ p.p.m.}$. 2-state fitting assumes only ES1 and 3-state fitting assumes both ES1 and ES2 for each resonance.

Supplementary Discussion

Remote RD is obscured by the active RD

A17, which is 3' to m¹A16, experiences a downfield shift in C1' (0.6 p.p.m.) and C8 (1.0 p.p.m.) in A₆DNA^{m1A16} relative to the unmodified duplex. While this is predicted to give rise to remote RD, the same nuclei also experience a downfield shift (3.3 p.p.m. and 2.2 p.p.m. respectively) due to active RD. However, RD profiles measured at A17 C1' and C8 at pH 6.8 did not call for a 3-state fit; rather they could be satisfactorily fit to a 2-state model yielding populations p_B (0.2%) and k_{ex} (600 s⁻¹) that are consistent with active RD at A17 and that are distinct from exchange parameters measured in the neighboring A16 (p_B ~0.4% and k_{ex} 3000 s⁻¹). Indeed, Bloch-McConnell simulations show that in part due to the similar signs of Δω, the smaller remote contribution to RD is obscured by the much larger contribution due to active RD (Supplementary Figure 11). In contrast, A17 C1' and C8 are both broadened out of detection in A₂-DNA^{m1A16}. Similarly, G10 C3', which is predicted to experience active RD due to the formation of G10-C15⁺ Hoogsteen bp and remote RD due to the formation of neighbor A16-T9 Hoogsteen bp at low pH, only lead to two-state rather than three-state behavior (Supplementary Figure 11).

Supplementary Table

Supplementary Table 1. BMRB entries with canonical DNA sugar chemical shifts used in this study

BMRB	PDB	Molecular type	¹³ C chemical shift	Sequence	Secondary structure
17129	2L5K	MUC1 DNA Aptamer	C1', C3', C4'	GCAGTTGATCCT TTGGATACCCCTGG	(((((((((...))))))))
15898	2K71	DNA GAAA Tetraloop	C1', C3', C4'	GCGAAAGC	((....))
5282	1PQT	DNA GAA loop	C1', C3', C4'	GCGAAGC	((...))
4103	---	BS2 Operator	C1', C3', C4'	d(GAAAGCCATTAGAG)	(((((((((((())))))))))))
15527	---	MBP1 Duplex	C1', C3', C4'	d(CTTACCGCGTCATTG)	(((((((((((())))))))))))
30254	5UZF	A6-DNA Duplex	C1', C3', C4'	d(CGATTTTTGGC)	(((((((((((())))))))))))
30253	5UZD	A2-DNA Duplex	C1', C3', C4'	d(GCATCGATTGGC)	(((((((((((())))))))))))
17887	2LIB	Alpha Anomeric Lesion	C1', C3'	d(GTCC <u>X</u> GGACG)	((((.-((((()))))))))
17409 ^a	2L8I	Triazole DNA Duplex	C1', C3'	d(GCTGCAA <u>AC</u> GTCTG)	(((((.-((((())))))).))))

a. Chemical shifts add 2.7 ppm to correct the entry using TMS as reference standard³.

Supplementary Table 2. Spin lock power and offsets used in the RD measurement from Bruker Avance III 700 MHz spectrometers

Nuclei	[spin lock power] {offset frequencies} [ω_{SL} 2 π^{-1} (s $^{-1}$)] { Ω 2 π^{-1} (s $^{-1}$)}
A₆-DNA pH 6.8	
A16-C1'	<ul style="list-style-type: none"> [150, 200, 250, 300, 350, 400, 500, 600, 700, 900, 1000, 1400, 1600, 1800, 2000, 2500, 3000, 3500] {0} [200] {-600, -500, -400, -350, -300, -250, -200, -150, -100, -50, 50, 100, 150, 200, 250, 300, 350, 400, 500, 600} [400] {-1200, -1050, -900, -750, -600, -450, -300, -200, -150, -50, 50, 150, 200, 300, 450, 600, 750, 900, 1050, 1200} [600] {-1800, -1600, -1400, -1200, -1000, -800, -600, -500, -400, -300, -200, -50, 50, 200, 400, 600, 1000, 1400, 1800} [1000] {-3000, -2500, -2000, -1500, -1000, -500, -300, -100, 100, 300, 500, 1000, 1500, 2000, 2500, 3000}
A16-C8	<ul style="list-style-type: none"> [150, 200, 250, 300, 400, 500, 600, 700, 900, 1000, 1200, 1400, 1600, 2000, 2500] {0} [200] {-600, -560, -520, -480, -440, -400, -360, -320, -280, -240, -200, -160, -120, -80, -40, 40, 120, 200, 300, 400, 500, 600} [400] {-1200, -800, -600, -500, -400, -350, -300, -250, -200, -150, -100, -50, 50, 100, 150, 200, 300, 400, 600, 800, 1000, 1200} [600] {-1800, -1500, -1000, -800, -650, -550, -450, -375, -300, -225, -150, -75, 75, 150, 225, 300, 375, 450, 550, 650, 800, 1000, 1500, 1800} [1000] {-2500, -2000, -1600, -1200, -900, -700, -600, -500, -400, -300, -200, -100, 100, 200, 300, 400, 500, 600, 700, 900, 1200, 1600, 2000, 2500}
A16-C3'	<ul style="list-style-type: none"> [150] {-300, -100, 280, 320, 360, 400, 400, 440} [200] {-600, -400, -200, -100, 100, 150, 200, 250, 300, 350, 400, 400, 450, 500, 550, 600} [400] {-1200, -1000, -800, -650, -500, -350, -200, -50, 100, 150, 200, 250, 300, 350, 400, 400, 450, 500, 550, 600, 650, 700, 850, 1000, 1150} [600] {-1800, -1400, -1000, -600, -400, -200, 100, 200, 250, 300, 350, 400, 400, 450, 500, 550, 600, 700, 800, 1000, 1200, 1400, 1800} [1000] {-2000, -1400, -800, -500, -200, 100, 250, 350, 400, 400, 450, 550, 700, 1000, 1300, 1600, 2200}
A16-C4'	<ul style="list-style-type: none"> [150, 200, 250, 300, 400, 500, 600, 700, 900, 1000, 1200, 1400, 1600, 2000, 2500] {0} [150] {-400, -300, -200, -100, -50, 40, 80, 120, 160, 200, 240, 280, 320, 360, 400, 440} [200] {-600, -500, -400, -300, -200, -120, -40, 40, 80, 120, 160, 200, 240, 280, 320, 360, 400, 440, 480, 520, 560, 600} [400] {-1200, -1000, -800, -600, -400, -300, -200, -150, -100, -50, 50, 100, 150, 200, 250, 300, 350, 400, 500, 600, 800, 1200} [600] {-1800, -1500, -1000, -800, -650, -550, -450, -375, -300, -225, -150, -75, 75, 150, 225, 300, 375, 450, 550, 650, 800, 1000, 1500, 1800} [1000] {-2500, -2000, -1600, -1200, -900, -700, -600, -500, -400, -300, -200, -100, 100, 200, 300, 400, 500, 600, 900, 1200, 1600, 2000, 2500}
T9-C3'	<ul style="list-style-type: none"> [150, 200, 250, 300, 400, 500, 600, 700, 900, 1000, 1200, 1400, 1600, 2000, 2500] {0} [200] {-600, -500, -400, -350, -300, -250, -200, -150, -100, -50, 50, 100, 150, 200, 250, 300, 350, 400, 500, 600} [400] {-1200, -1050, -900, -600, -450, -300, -250, -200, -150, -100, -50, 50, 100, 150, 200, 250, 300, 450, 600, 750, 900, 1050, 1200} [600] {-1800, -1400, -1000, -800, -600, -400, -300, -200, -150, -100, -50, 50, 100, 150, 200, 300, 400, 600, 800, 1000, 1400, 1800} [1000] {-2400, -1800, -1200, -900, -600, -300, -150, -50, 50, 150, 300, 600, 900, 1200, 1800, 2400}

C15-C3'	[150, 200, 250, 300, 400, 500, 600, 700, 900, 1000, 1200, 1400, 1600, 2000, 2500] {0} [200] {-600, -500, -400, -350, -300, -250, -200, -150, -100, -50, 50, 100, 150, 200, 250, 300, 350, 400, 500, 600} [400] {-1000, -800, -600, -500, -400, -350, -300, -250, -200, -150, -100, -50, 50, 100, 150, 200, 250, 300, 350, 400, 500, 600} [600] {-1800, -1400, -1200, -1000, -800, -600, -400, -300, -200, -100, -50, 50, 100, 200, 300, 400, 600, 800, 1000, 1200, 1400, 1800} [1000] {-3000, -3000, -2500, -2500, -2000, -1500, -1200, -900, -600, -300, -150, -50, 50, 150, 300, 600, 900, 1200, 1500, 2000, 3000}
G10-C3'	[150, 200, 250, 300, 400, 500, 600, 700, 900, 1000, 1200, 1400, 1600, 2000, 2500] {0} [200] {-600, -350, -300, -250, -200, -150, -100, -50, 50, 100, 150, 200, 250, 300, 350, 600} [400] {-1200, -1050, -900, -600, -450, -300, -250, -200, -150, -100, -50, 50, 100, 150, 200, 250, 300, 450, 600, 750, 900, 1050, 1200} [600] {-1800, -1400, -1000, -800, -600, -400, -300, -200, -150, -100, -50, 50, 100, 150, 200, 300, 400, 600, 800, 1000, 1400, 1800} [1000] {-2400, -1800, -1200, -900, -600, -300, -150, -50, 50, 150, 300, 600, 900, 1200, 1800, 2400}
A₆-DNA pH 5.4	
A16-C1'	[150, 200, 250, 300, 400, 500, 600, 700, 900, 1000, 1200, 1400, 1600, 2000, 2500] {0} [200] {-600, -550, -500, -450, -400, -350, -300, -250, -200, -150, -100, -50, 50, 100, 150, 200, 300, 400, 600} [400] {-1100, -950, -800, -650, -500, -450, -400, -350, -300, -250, -200, -150, -100, -50, 50, 100, 250, 400, 550, 700, 850, 1000, 1200} [600] {-1600, -1200, -1000, -800, -600, -500, -400, -350, -300, -250, -200, -150, -100, -50, 100, 200, 400, 600, 800, 1200, 1600} [1000] {-2000, -1400, -1100, -800, -500, -350, -250, -200, -150, -100, -50, 100, 400, 700, 1000, 1600, 2200}
A16-C8	[150, 200, 250, 300, 400, 500, 600, 700, 900, 1000, 1200, 1400, 1600, 2000, 2500] {0} [200] {-600, -550, -500, -450, -400, -350, -300, -250, -200, -150, -100, -50, 50, 100, 150, 200, 300, 400} [400] {-1100, -950, -800, -650, -500, -450, -400, -350, -300, -250, -200, -150, -100, -50, 50, 100, 250, 400, 550, 700, 850, 1000, 1200} [600] {-1600, -1200, -1000, -800, -600, -500, -400, -350, -300, -250, -200, -150, -100, -50, 100, 200, 400, 600, 800, 1200, 1600} [1000] {-2000, -1400, -1100, -800, -500, -350, -250, -200, -150, -100, -50, 100, 400, 700, 1000, 1600, 2200}
G10-C1'	[150, 200, 250, 300, 400, 500, 600, 700, 900, 1000, 1200, 1400, 1600, 2000, 2500] {0} [200] {-600, -550, -500, -450, -400, -350, -300, -250, -200, -150, -100, -50, 100, 200, 400, 600} [400] {-1150, -1000, -850, -700, -650, -600, -550, -500, -450, -400, -400, -350, -300, -250, -200, -150, -100, 50, 200, 350, 500, 650, 800, 1000, 1200} [600] {-1800, -1400, -1200, -1000, -800, -700, -600, -550, -500, -450, -400, -400, -350, -300, -250, -200, -150, -100, 200, 400, 600, 1000, 1400, 1800} [1000] {-2200, -1600, -1300, -1000, -700, -550, -450, -400, -400, -350, -250, -100, 200, 500, 800, 1400, 2000}
G10-C8	[150, 200, 250, 300, 400, 500, 600, 700, 900, 1000, 1200, 1400, 1600, 2000, 2500] {0} [150] {-440, -400, -400, -360, -320, -280, -240, -200, -160, -120, -60, 100, 300} [200] {-600, -550, -500, -450, -400, -400, -350, -300, -250, -200, -150, -100, -50, 100, 200, 400, 600} [400] {-1150, -1000, -850, -700, -650, -600, -550, -500, -450, -400, -400, -350, -300, -250, -200, -150, -100, 50, 200, 350, 500, 650, 800, 1000, 1200} [600] {-1800, -1400, -1200, -1000, -800, -700, -600, -550, -500, -450, -400, -400, -350, -300, -250, -200, -150, -100, 200, 400, 600, 1000, 1400, 1800}
G10-C3'	[150, 200, 250, 300, 400, 500, 600, 700, 900, 1000, 1200, 1400, 1600, 2000, 2500] {0} [200] {-600, -400, -200, -100, 50, 100, 150, 200, 250, 300, 350, 400, 400, 450, 500, 550, 600} [300] {-800, -600, -400, -200, -100, 50, 100, 150, 200, 250, 300, 350, 400, 400, 450, 500, 550, 600, 650, 700, 750, 800, 900} [400] {-1200, -1000, -800, -650, -500, -350, -200, -50, 100, 150, 200, 250, 300, 350, 400, 400, 450, 500, 550, 600, 500, 550, 600, 650, 700, 850, 1000, 1150} [600] {-1800, -1400, -1000, -600, -400, -200, 100, 200, 250, 300, 350, 400, 400, 450, 500, 550, 600, 700, 800, 1000, 1200, 1400, 1800} [1000] {-2400, -1800, -1200, -900, -600, -300, -150, -50, 50, 150, 300, 600, 900, 1200, 1800, 2400}

A ₂ -DNA pH 5.4	
A16-C1'	[150, 200, 250, 300, 400, 500, 600, 700, 900, 1000, 1200, 1400, 1600, 2000, 2500] {0} [200] {-400, -400, -350, -300, -250, -200, -150, -100, -50, 100, 200, 400, 600} [400] {-1150, -1000, -850, -700, -650, -600, -550, -500, -450, -400, -400, -350, -300, -250, -200, -150, -100, 50, 200, 350, 500, 650, 800, 1000, 1200} [600] {-1800, -1400, -1200, -1000, -800, -700, -600, -550, -500, -450, -400, -400, -350, -300, -250, -200, -100, 200, 400, 600, 1000, 1400, 1800} [1000] {-2200, -1600, -1300, -1000, -700, -550, -450, -400, -400, -350, -250, -100, 200, 500, 800, 1400, 2000}
A16-C8	[150, 200, 250, 300, 400, 500, 600, 700, 900, 1000, 1200, 1400, 1600, 2000, 2500] {0} [200] {-400, -400, -350, -300, -250, -200, -150, -100, -50, 100, 200, 400, 600} [400] {-1150, -1000, -850, -700, -650, -600, -550, -500, -450, -400, -400, -350, -300, -250, -200, -150, -100, 50, 200, 350, 500, 650, 800, 1000, 1200} [600] {-1800, -1400, -1200, -1000, -800, -700, -600, -550, -500, -450, -400, -400, -350, -300, -250, -200, -100, 200, 400, 600, 1000, 1400, 1800} [1000] {-2200, -1600, -1300, -1000, -700, -550, -450, -400, -400, -350, -250, -100, 200, 500, 800, 1400, 2000}
A16-C3'	[150, 200, 250, 300, 400, 500, 600, 700, 900, 1000, 1200, 1400, 1600, 2000, 2500] {0} [150] {-300, -100, 60, 120, 160, 200, 240, 280, 320, 360, 400, 400, 440} [200] {-600, -400, -200, -100, 50, 100, 150, 200, 250, 300, 350, 400, 400, 450, 500, 550, 600} [400] {-1200, -1000, -800, -650, -500, -350, -200, -50, 100, 150, 200, 250, 300, 350, 400, 400, 450, 500, 550, 600, 650, 700, 850, 1000, 1150} [600] {-1800, -1400, -1000, -600, -400, -200, 100, 200, 250, 300, 350, 400, 400, 450, 500, 550, 600, 700, 800, 1000, 1200, 1400, 1800} [1000] {-2000, -1400, -800, -500, -200, 100, 250, 350, 400, 400, 450, 550, 700, 1000, 1300, 1600, 2200}
A16-C4'	[150, 200, 250, 300, 400, 500, 600, 700, 900, 1000, 1200, 1400, 1600, 2000, 2500] {0} [150] {-400, -340, -280, -240, -200, -160, -120, -80, -40, 40, 80, 120, 160, 200, 240, 280, 340, 400} [200] {-600, -500, -400, -350, -300, -250, -200, -150, -100, -50, 50, 100, 150, 200, 250, 300, 350, 400, 500, 600} [400] {-1200, -1050, -900, -750, -600, -450, -300, -250, -200, -150, -100, -50, 50, 100, 150, 200, 250, 300, 450, 600, 750, 900, 1050, 1200} [600] {-1800, -1400, -1000, -800, -600, -400, -300, -200, -150, -100, -50, 50, 100, 150, 200, 300, 400, 600, 800, 1000, 1400, 1800} [1000] {-2400, -1800, -1200, -900, -600, -300, -150, -50, 50, 150, 300, 600, 900, 1200, 1800, 2400}
T9-C3'	[200, 250, 300, 400, 500, 600, 700, 900, 1000, 1200, 1400, 1600, 2000, 2500] {0} [150] {-400, -340, -280, -240, -200, -160, -120, -80, -40, 40, 80, 120, 160, 200, 240, 280, 340, 400} [200] {-600, -500, -400, -350, -300, -250, -200, -150, -100, -50, 50, 100, 150, 200, 250, 300, 350, 400, 500, 600} [400] {-1200, -1050, -900, -600, -450, -300, -250, -200, -150, -100, -50, 50, 100, 150, 200, 250, 300, 450, 600, 750, 900, 1050, 1200} [600] {-1800, -1400, -1000, -800, -600, -400, -300, -200, -150, -100, -50, 50, 100, 150, 200, 300, 400, 600, 800, 1000, 1400, 1800} [1000] {-2400, -1800, -1200, -900, -600, -300, -150, -50, 50, 150, 300, 600, 900, 1200, 1800, 2400}
C15-C6	[200, 250, 300, 400, 500, 600, 700, 900, 1000, 1200, 1400, 1600, 2000, 2500] {0} [150] {-340, -280, -240, -200, -160, -120, -80, -40, 40, 80, 120, 160, 200, 240, 280, 340, 400} [200] {-600, -500, -400, -350, -300, -250, -200, -150, -100, -50, 50, 100, 150, 200, 250, 300, 350, 400, 500, 600} [400] {-1200, -900, -750, -600, -450, -300, -250, -200, -150, -100, -50, 50, 100, 150, 200, 250, 300, 450, 600, 750, 900, 1050, 1200} [600] {-1800, -1400, -1000, -800, -600, -400, -300, -200, -150, -100, -50, 50, 100, 150, 200, 300, 400, 600, 800, 1000, 1400, 1800}

C14-C3'	[150, 200, 250, 300, 400, 500, 600, 700, 900, 1000, 1200, 1400, 1600, 2000, 2500] {0} [200] {-600, -500, -400, -350, -300, -250, -200, -150, -100, -50, 50, 100, 150, 200, 250, 300, 350, 400, 500, 600} [400] {-1200, -1050, -900, -750, -600, -450, -300, -250, -200, -150, -100, -50, 50, 100, 150, 200, 250, 300, 450, 600, 750, 900, 1050, 1200} [600] {-1800, -1400, -1000, -800, -600, -400, -300, -200, -150, -100, -50, 50, 100, 150, 200, 300, 400, 600, 800, 1000, 1400, 1800} [1000] {-2400, -1800, -1200, -900, -300, -150, -50, 50, 150, 300, 600, 900, 1200, 1800, 2400}
---------	--

Supplementary Table 3. Exchange parameters from globally fitting ^{13}C RD data in A₆-DNA

Res	pH	$\Delta\omega_B$ (ppm)	$\Delta\omega_C$ (ppm)	p_B (%)	p_c (%)	k_{exAB} (s^{-1})	k_{exAC} (s^{-1})	R_1 (s^{-1})	R_2 (s^{-1})
A16-C8	6.8	2.27±0.06	N/A	0.45±0.01	N/A	2885±84	N/A	1.43±0.07	27.58±0.14
A16-C1'		3.01±0.07						1.20±0.06	17.92±0.13
A16-C3'		-3.52±0.06						1.38±0.07	17.25±0.18
A16-C4'		-2.22±0.07						1.42±0.09	17.46±0.16
T9-C3'		-1.89±0.14						1.22±0.16	16.43±0.31
C15-C3'		2.66±0.05						1.37±0.04	13.90±0.10
G10-C3'		1.03±0.05						1.31±0.05	17.21±0.09
G10-C8		3.03±0.07	N/A	0.40±0.01	N/A	992±52	N/A	1.45±0.07	27.42±0.11
G10-C1'		3.56±0.09						1.22±0.08	18.09±0.10
G10-C3'		-2.70±0.05						1.45±0.05	18.25±0.07
G10-C4'		-1.66±0.05						1.43±0.04	16.44±0.06
C15-C6		2.59±0.21						1.93±0.16	38.52±0.21
G11-C8		0.72±0.07						1.44±0.05	27.87±0.07
G11-C3'		1.25±0.04						1.39±0.04	16.20±0.05
C14-C3'		1.32±0.07						1.49±0.06	14.87±0.08
C15-C3'		-1.81±0.07	2.70±0.07	0.49±0.02	N/A	2962±119	N/A	1.24±0.06	14.38±0.14
T9-C3'		2.18±0.12	-2.04±0.08					1.19±0.10	16.42±0.21
A16-C8		N/A	2.83±0.10					1.45±0.12	27.69±0.23
A16-C1'			3.40±0.10					1.40±0.11	18.03±0.22

Supplementary Table 4. Exchange parameters from globally fitting ^{13}C RD data in A₂-DNA

Res	pH	$\Delta\omega_B$ (ppm)	$\Delta\omega_C$ (ppm)	p_B (%)	p_c (%)	k_{exAB} (s^{-1})	k_{exAC} (s^{-1})	R_1 (s^{-1})	R_2 (s^{-1})			
A16-C8	5.4	2.84±0.11	N/A	0.56±0.04	N/A	4847±161	N/A	1.36±0.09	29.43±0.26			
A16-C1'		2.93±0.10						1.28±0.08	18.79±0.23			
A16-C3'		-2.55±0.09						1.28±0.05	20.15±0.18			
A16-C4'		-1.64±0.06						1.18±0.04	18.86±0.12			
T9-C3'		-1.36±0.07	2.19±0.03	0.96±0.02	N/A	1339±36	N/A	1.09±0.06	18.60±0.14			
C15-C3'		2.22±0.07	-1.22±0.02					1.47±0.04	15.63±0.14			
G10-C8		N/A	3.28±0.04	N/A				1.13±0.10	30.70±0.15			
G10-C1'			3.62±0.06					0.70±0.13	20.53±0.18			
G10-C8	5.4	3.31±0.04	N/A	0.91±0.01	N/A	1412±24	N/A	1.19±0.10	30.68±0.14			
G10-C1'		3.63±0.06						0.78±0.13	20.55±0.16			
G10-C3'		-2.54±0.02						1.14±0.05	19.26±0.08			
G10-C4'		-1.06±0.02						1.33±0.04	18.22±0.05			
C15-C6		2.51±0.08						1.34±0.14	40.13±0.23			
G11-C8		0.71±0.02						1.24±0.04	32.09±0.06			
G11-C3'		0.91±0.02	N/A	0.40±0.03	N/A	4304±188	N/A	1.47±0.04	17.13±0.06			
C14-C3'		0.97±0.02						1.25±0.03	16.07±0.05			
C15-C3'		-1.30±0.02	2.51±0.09					1.41±0.04	15.89±0.14			
T9-C3'		2.27±0.03	-1.52±0.08					1.09±0.05	18.63±0.13			
A16-C8		N/A	3.24±0.12	N/A				1.26±0.09	30.02±0.25			
A16-C1'			3.43±0.12					1.14±0.08	19.25±0.23			

Reference

1. Ulrich, E.L. et al. BioMagResBank. *Nucleic Acids Res* **36**, D402-8 (2008).
2. Sathyamoorthy, B. et al. Insights into Watson-Crick/Hoogsteen breathing dynamics and damage repair from the solution structure and dynamic ensemble of DNA duplexes containing m1A. *Nucleic Acids Res* (2017).
3. Aeschbacher, T., Schubert, M. & Allain, F.H. A procedure to validate and correct the ¹³C chemical shift calibration of RNA datasets. *J Biomol NMR* **52**, 179-90 (2012).